Study of the branching ratio and charge asymmetry for the decay $K_S \to \pi e \nu$ with the KLOE detector

The KLOE Collaboration

F. Ambrosino [e], A. Antonelli [b] M. Antonelli [b], C. Bacci [i], P. Beltrame [c], G. Bencivenni [b], S. Bertolucci [b], C. Bini [g], C. Bloise [b], V. Bocci [g], F. Bossi [b], D. Bowring [a], P. Branchini [i], R. Caloi [g], P. Campana [b], G. Capon [b], T. Capussela [e], F. Ceradini [i], S. Chi [b], G. Chiefari [e], P. Ciambrone [b], S. Conetti [a], E. De Lucia [b], A. De Santis [g], P. De Simone [b], G. De Zorzi [g], S. Dell'Agnello [b], A. Denig [c], A. Di Domenico [g], C. Di Donato [e], S. Di Falco [j], B. Di Micco [i], A. Doria [e], M. Dreucci [b], G. Felici [b], A. Ferrari [b], M. L. Ferrer [b], G. Finocchiaro [b], S. Fiore [g], C. Forti [b], P. Franzini [g], C. Gatti [b,1], P. Gauzzi [g], S. Giovannella [b], E. Gorini [d], E. Graziani [i], M. Incagli [j], W. Kluge [c], V. Kulikov [m], F. Lacava [g], G. Lanfranchi [b], J. Lee-Franzini [b,k], D. Leone [c], M. Martini [b], P. Massarotti [e], W. Mei [b], S. Meola [e], S. Miscetti [b], M. Moulson [b], S. Müller [b,c], F. Murtas [b], M. Napolitano [e], F. Nguyen [i], M. Palutan [b], E. Pasqualucci [g], A. Passeri [i], V. Patera [b,f], F. Perfetto [e], L. Pontecorvo [g], M. Primavera [d], P. Santangelo [b], E. Santovetti [h], G. Saracino [e], B. Sciascia [b], A. Sciubba [b,f], F. Scuri [j], I. Sfiligoi [b], T. Spadaro [b,2], M. Testa [g], L. Tortora [i], P. Valente [b], B. Valeriani [c], G. Venanzoni [b], S. Veneziano [g], A. Ventura [d], R. Versaci [b], G. Xu [b,ℓ],

[a] *Physics Department, University of Virginia, Charlottesville, VA, USA.*

[b] *Laboratori Nazionali di Frascati dell'INFN, Frascati, Italy.*

[c] *Institut für Experimentelle Kernphysik, Universität Karlsruhe, Germany.*

[d] *Dipartimento di Fisica dell'Università e Sezione INFN, Lecce, Italy.*

[e] *Dipartimento di Scienze Fisiche dell'Università "Federico II" e Sezione INFN, Napoli, Italy*

[f] *Dipartimento di Energetica dell'Università "La Sapienza", Roma, Italy.*

Preprint submitted to Elsevier Science *7 February 2008*

[g] *Dipartimento di Fisica dell'Università "La Sapienza" e Sezione INFN, Roma, Italy.*

[h] *Dipartimento di Fisica dell'Università "Tor Vergata" e Sezione INFN, Roma, Italy.*

[i] *Dipartimento di Fisica dell'Università "Roma Tre" e Sezione INFN, Roma, Italy.*

[j] *Dipartimento di Fisica dell'Università e Sezione INFN, Pisa, Italy.*

[k] *Physics Department, State University of New York at Stony Brook, NY, USA.*

[ℓ] *Permanent address: Institute of High Energy Physics, CAS, Beijing, China.*

[m] *Permanent address: Institute for Theoretical and Experimental Physics, Moscow, Russia.*

[1] Corresponding author: Claudio Gatti INFN - LNF, Casella postale 13, 00044 Frascati (Roma), Italy; tel. +39-06-94032727, e-mail claudio.gatti@lnf.infn.it

[2] Corresponding author: Tommaso Spadaro INFN - LNF, Casella postale 13, 00044 Frascati (Roma), Italy; tel. +39-06-94032698, e-mail tommaso.spadaro@lnf.infn.it

Abstract

Among some 400 million K_SK_L pairs produced in e^+e^- annihilations at DAΦNE, $\sim$6500 each of $K_S \to \pi^+e^-\bar{\nu}$ and $K_S \to \pi^-e^+\nu$ decays have been observed with the KLOE detector. From these, the ratio $\Gamma(K_S \to \pi e\nu)/\Gamma(K_S \to \pi^+\pi^-) = (10.19 \pm 0.13) \times 10^{-4}$ is obtained, improving the accuracy on $\mathrm{BR}(K_S \to \pi e\nu)$ by a factor of four and providing the most precise test of the $\Delta S = \Delta Q$ rule. From the partial width $\Gamma(K_S \to \pi e\nu)$, a value for $f_+^{K^0}(0) \times V_{us}$ is obtained that is in agreement with unitarity of the quark-mixing matrix. The lepton charge asymmetry $A_S = (1.5 \pm 9.6_{\mathrm{stat}} \pm 2.9_{\mathrm{syst}}) \times 10^{-3}$ is compatible with the requirements of CPT invariance. The form-factor slope agrees with recent results from semileptonic K_L and K^+ decays. These are the first measurements of the charge asymmetry and form-factor slope for semileptonic K_S decays.

1 Introduction

Semileptonic kaon decays provide at present the best way to learn about s, u quark couplings and allow tests of many fundamental aspects of the Standard Model (SM). Only the vector part of the weak current has a non-vanishing matrix element between a kaon and a pion. The vector current is "almost" conserved. For a vector interaction, there are no $SU(3)$-breaking corrections to first order in the s-d mass difference [1], making calculations of hadronic matrix elements more reliable. Therefore, the CKM matrix element V_{us} can be accurately extracted from the measurement of the semileptonic decay widths

and the most precise test of unitarity of the CKM matrix can be obtained from the first-row constraint: $1-\Delta \simeq |V_{ud}|^2+|V_{us}|^2$. Using V_{ud} from $0^+ \to 0^+$ nuclear beta decays, a test of the expectation $\Delta = 0$ with a precision of one part per mil can be performed.

At a ϕ factory very large samples of tagged, monochromatic K_S mesons are available. We have isolated a very pure sample of $\sim$13 000 semileptonic K_S decay events and measured for the first time the partial decay rates for transitions to final states of each charge, $\Gamma(K_S \to e^+\pi^-\nu)$ and $\Gamma(K_S \to e^-\pi^+\bar{\nu})$, and the charge asymmetry

$$A_S = \frac{\Gamma\left(K_S \to \pi^- e^+ \nu\right) - \Gamma\left(K_S \to \pi^+ e^- \bar{\nu}\right)}{\Gamma\left(K_S \to \pi^- e^+ \nu\right) + \Gamma\left(K_S \to \pi^+ e^- \bar{\nu}\right)}. \tag{1}$$

The comparison of A_S with the asymmetry A_L for K_L decays allows tests of the CP and CPT symmetries. Comparison of the K_S and K_L widths $\Gamma(K_S \to \pi e \nu)$ and $\Gamma(K_L \to \pi e \nu)$ allows a test of the validity of the $\Delta S = \Delta Q$ rule. Assuming CPT invariance, $A_S = A_L = 2\,\mathrm{Re}\,\epsilon \simeq 3 \times 10^{-3}$, where ϵ gives the CP impurity of the K_S, K_L mass eigenstates due to CP violation in $K \leftrightarrow \overline{K}$ $\Delta S = 2$ transitions. The difference between the charge asymmetries,

$$A_S - A_L = 4\,\left(\mathrm{Re}\,\delta + \mathrm{Re}\,x_-\right), \tag{2}$$

signals CPT violation either in the mass matrix (δ term), or in the decay amplitudes with $\Delta S \neq \Delta Q$ (x_- term). The sum of the asymmetries,

$$A_S + A_L = 4\,\left(\mathrm{Re}\,\epsilon - \mathrm{Re}\,y\right), \tag{3}$$

is related to CP violation in the mass matrix (ϵ term) and to CPT violation in the $\Delta S = \Delta Q$ decay amplitude (y term). Finally, the validity of the $\Delta S = \Delta Q$ rule in CPT-conserving transitions can be tested through the quantity:

$$\mathrm{Re}\,x_+ = \frac{1}{2}\frac{\Gamma(K_S \to \pi e \nu) - \Gamma(K_L \to \pi e \nu)}{\Gamma(K_S \to \pi e \nu) + \Gamma(K_L \to \pi e \nu)}. \tag{4}$$

Writing the K^0 and $\overline{K}^0$ decay amplitudes for final states of each charge as $\mathcal{A}_\pm = A(K^0 \to e^\pm \pi^\mp \nu(\bar{\nu}))$ and $\bar{\mathcal{A}}_\pm = A(\overline{K}^0 \to e^\pm \pi^\mp \nu(\bar{\nu}))$, the above parameters are defined as follows:

$$\begin{aligned} x_\pm &= \frac{1}{2}\left[\frac{\bar{\mathcal{A}}_+}{\mathcal{A}_+} \pm \left(\frac{\mathcal{A}_-}{\bar{\mathcal{A}}_-}\right)^*\right], \\ y &= \frac{\bar{\mathcal{A}}_-^* - \mathcal{A}_+}{\bar{\mathcal{A}}_-^* + \mathcal{A}_+}, \end{aligned} \tag{5a}$$

$$\epsilon = i\frac{\mathrm{Im}M_{12} - i\mathrm{Im}\Gamma_{12}/2}{m_S - m_L - i(1/\tau_S - 1/\tau_L)/2},$$
$$\delta = \frac{1}{2}\frac{M_{11} - M_{22} - i(\Gamma_{11} - \Gamma_{22})/2}{m_S - m_L - i(1/\tau_S - 1/\tau_L)/2}, \tag{5b}$$

where M_{ij} and Γ_{ij} are the elements of the mass and decay matrices describing the time evolution of the neutral kaon system, and $m_{S,L}$ and $\tau_{S,L}$ are respectively the masses and lifetimes for $K_{S,L}$.

The value of A_L is known at present with an accuracy of 10^{-4} [2], while A_S has never yet been measured. At present, the most precise test of CPT conservation comes from the CPLEAR experiment [3]: they find $\mathrm{Re}\,\delta$ and $\mathrm{Re}\,x_-$ to be compatible with zero, with accuracies of 3×10^{-4} and 10^{-2}, respectively. The present value of $\mathrm{Re}\,y$, obtained from unitarity [4], is compatible with zero to within 3×10^{-3}.

In the SM, $\mathrm{Re}\,x_+$ is on the order of $G_F m_\pi^2 \sim 10^{-7}$, being due to second-order weak transitions. At present, the most precise test of the $\Delta S = \Delta Q$ rule comes from an analysis of the time distribution of strangeness-tagged semileptonic kaon decays at CPLEAR [5]. They found $\mathrm{Re}\,x_+$ to be compatible with zero to within 6×10^{-3}.

The most precise previous measurement of $\mathrm{BR}(K_S \to \pi e\nu)$ was obtained by KLOE using $\sim 20\mathrm{pb}^{-1}$ of data collected in 2000 and has a fractional accuracy of 5.4% [6]. The present result is based on the analysis of 410 pb^{-1} of data and improves on the total error by a factor of four, to 1.3%.

2 Measurement method

We measure K_S branching ratios using kaons from $\phi \to K_S K_L$ decays. The data were collected with the KLOE detector at DAΦNE, the Frascati ϕ-factory. DAΦNE is an e^+e^- collider that operates at a center of mass energy of $\sim$1020 MeV, the mass of the ϕ meson. Equal-energy positron and electron beams collide at an angle of $\pi - 25$ mrad, producing ϕ mesons with a small momentum in the horizontal plane: $p_\phi \sim 13$MeV. ϕ mesons decay $\sim$34% of the time into neutral kaons. K_L's and K_S's have mean decay paths of $\lambda_L \sim 350$ cm and $\lambda_S \sim 0.6$ cm, respectively.

The KLOE detector consists of a large cylindrical drift chamber surrounded by a lead/scintillating-fiber sampling calorimeter. A superconducting coil outside the calorimeter provides a 0.52 T field. The drift chamber [7], which is 4 m in diameter and 3.3 m long, has 12 582 cells strung in all-stereo geometry. The chamber shell is made of a carbon-fiber/epoxy composite. The chamber is filled

with a 90% He, 10% iC_4H_{10} mixture. These features maximize transparency to photons and reduce $K_L \to K_S$ regeneration. The spatial resolutions are $\sigma_{xy} \sim 150\,\mu$m and $\sigma_z \sim 2\,$mm. The momentum resolution is $\sigma_{p_\perp)}/p_\perp \leq 0.4\%$. Vertices are reconstructed with a spatial resolution of $\sim 3\,$mm. The calorimeter [8] is divided into a barrel and two endcaps and covers 98% of the solid angle. The energy resolution is $\sigma_E/E = 5.7\%/\sqrt{E(\mathrm{GeV})}$ and the timing resolution is $\sigma_t = 57\,\mathrm{ps}/\sqrt{E(\mathrm{GeV})} \oplus 100\,\mathrm{ps}$ [9]. The trigger used for the present analysis relies entirely on calorimeter information [10]. Two local energy deposits above threshold (50 MeV on the barrel, 150 MeV on the endcaps) are required. The trigger time has a large spread with respect to the bunch-crossing period. However, it is synchronized with the machine RF divided by 4, $T_{\mathrm{sync}} \sim 10.8\,$ns, with an accuracy of 50 ps. As a result, the time T_0 of the bunch crossing producing an event, which is determined after event reconstruction, is known up to an integer multiple of the bunch-crossing time, $T_{\mathrm{bunch}} \sim 2.7\,$ns.

The main advantage of studying kaons at a ϕ factory is that K_L's and K_S's are produced nearly back-to-back in the laboratory so that detection of a K_L meson tags the production of a K_S meson and gives its direction and momentum. The contamination from $K_L K_L \gamma$ and $K_S K_S \gamma$ final states is negligible for our measurement [11, 12]. Since the branching ratio for $K_S \to \pi^+\pi^-$ is known with an accuracy of $\sim 0.1\%$ [13, 14], the $K_S \to \pi e \nu$ branching ratio is evaluated by normalizing the number of signal events, separately for each charge state, to the number of $K_S \to \pi^+\pi^-$ events in the same data set. This allows cancellation of the uncertainties arising from the integrated luminosity, the ϕ production cross section, and the tagging efficiency. The measurement is based on an integrated luminosity of $410\,\mathrm{pb}^{-1}$ at the ϕ peak collected during two distinct data-taking periods in the years 2001 and 2002, corresponding to $\sim 1.3 \times 10^9$ produced ϕ-mesons. Since the machine conditions were different during the two periods, we have measured the branching ratios separately for each data set. Our final results are based on the averages of these measurements.

3 Selection criteria

About half of the K_L mesons reach the calorimeter, where most interact. Such an interaction is called a K_L *crash* in the following. A K_L crash is identified as a local energy deposit with $E > 200\,$MeV and a time of flight corresponding to a low velocity: $\beta \sim 0.216$. The coordinates of the energy deposit determine the K_L direction to within $\sim 20\,$mrad, as well as the momentum $\mathbf{p}_L$, which is weakly dependent on the K_L direction because of the motion of the ϕ meson. A K_L crash thus tags the production of a K_S of momentum $\mathbf{p}_S = \mathbf{p}_\phi - \mathbf{p}_L$. K_S mesons are tagged with an overall efficiency of $\sim 20\%$. Both $K_S \to \pi e \nu$

	Year 2001	Year 2002
Luminosity, pb^{-1}	152 ± 1	286 ± 2
Channel	Number of selected events	
$K_S \to \pi^+\pi^-$	13 056 500	22 840 700
$K_S \to \pi^+ e^- \bar{\nu}$	$2387 \pm 52_{\mathrm{stat}} \pm 22_{\mathrm{syst}}$	$4238 \pm 69_{\mathrm{stat}} \pm 55_{\mathrm{syst}}$
$K_S \to \pi^- e^+ \nu$	$2541 \pm 52_{\mathrm{stat}} \pm 24_{\mathrm{syst}}$	$4446 \pm 71_{\mathrm{stat}} \pm 69_{\mathrm{syst}}$

Table 1
Number of selected $K_S \to \pi^+\pi^-$ and $K_S \to \pi e \nu$ decays for the 2001 and 2002 data sets.

and $K_S \to \pi^+\pi^-$ decays are selected from this tagged sample. Event selection consists of fiducial cuts, particle identification by time of flight, and kinematic closure.

Identification of a $K_S \to \pi^+\pi^-$ decay requires two tracks of opposite curvature. The tracks must extrapolate to the interaction point (IP) to within a few centimeters. The reconstructed momenta and polar angles must lie in the intervals $120\,\mathrm{MeV} < p < 300\,\mathrm{MeV}$ and $30^\circ < \theta < 150^\circ$. A cut in $(p_\perp, p_\parallel)$ selects non-spiralling tracks. The numbers of $K_S \to \pi^+\pi^-$ events found in each data set are shown in Tab. 1. Contamination due to K_S decays other than $K_S \to \pi^+\pi^-$ is at the per-mil level and is estimated from Monte Carlo (MC).

Identification of a $K_S \to \pi e \nu$ event also begins with the requirement of two tracks of opposite curvature. The tracks must extrapolate *and form a vertex* close to the IP. The invariant mass $M_{\pi\pi}$ of the pair calculated assuming both tracks are pions must be smaller than 490 MeV. This rejects $\sim 95\%$ of the $\pi^+\pi^-$ decays and $\sim 10\%$ of the signal events.

We discriminate between electron and pion tracks by time of flight (TOF). The tracks are therefore required to be associated with calorimeter energy clusters. For each track, we compute the difference $\delta_t(m) = t_{\mathrm{cl}} - L/c\beta(m)$ using the cluster time t_{cl} and the track length L. The velocity β is computed from the track momentum for each mass hypothesis, $m = m_e$ and $m = m_\pi$. In order to avoid uncertainties due to the determination of T_0 (the time of the bunch crossing producing the event), we make cuts on the two-track difference

$$\mathrm{d}\delta_{t,ab} = \delta_t(m_a)_1 - \delta_t(m_b)_2,$$

where the mass hypothesis $m_{a(b)}$ is used for track 1(2). This difference is zero for the correct mass assignments. First, $K_S \to \pi^+\pi^-$ events are rejected by requiring $|\mathrm{d}\delta_{t,\pi\pi}| > 1.7\,\mathrm{ns}$. Then, the differences $\mathrm{d}\delta_{t,\pi e}$ and $\mathrm{d}\delta_{t,e\pi}$ are calculated for surviving events. The scatter plot of the two variables is shown in Fig. 1 for Monte Carlo events. The cuts applied on these time differences for the selection of $K_S \to \pi e \nu$ events are illustrated in the figure: $|\mathrm{d}\delta_{t,\pi e}| < 1.4\,\mathrm{ns}$, $\mathrm{d}\delta_{t,e\pi} > 3.2\,\mathrm{ns}$; or $|\mathrm{d}\delta_{t,e\pi}| < 1.4\,\mathrm{ns}$, $\mathrm{d}\delta_{t,\pi e} > 3.2\,\mathrm{ns}$. After these TOF requirements, particle types and charges for signal events can be assigned very precisely: the probability of

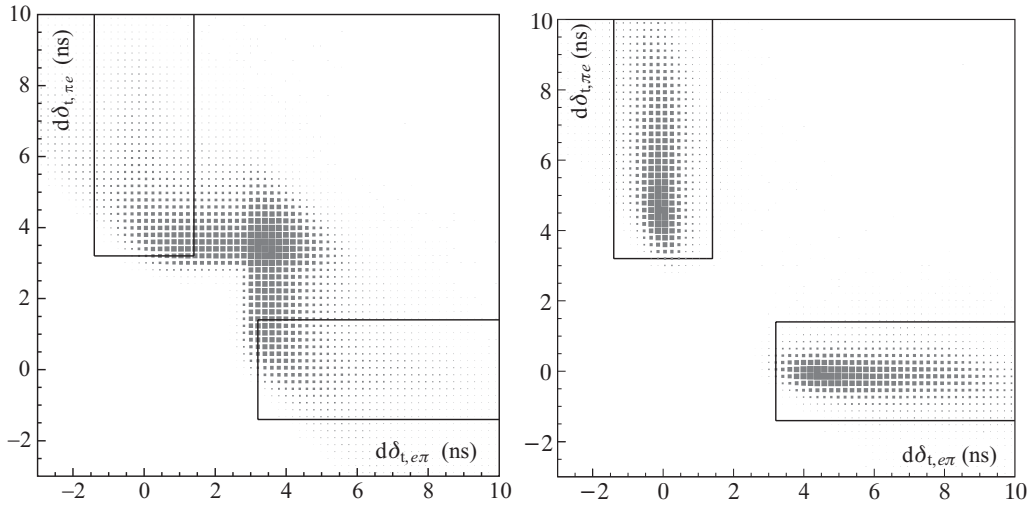

Fig. 1. Scatter plot of the time differences $d\delta_{t,\pi e}$ vs $d\delta_{t,e\pi}$ for Monte Carlo events, for all K_S decays (left) and for $K_S \to \pi e\nu$ decays (right).

misidentifying a $\pi^+ e^- \bar{\nu}$ event as $\pi^- e^+ \nu$ or vice versa is negligible. These cuts reject $\sim 90\%$ of the background events, while the efficiency for the signal is $\sim 85\%$.

Once particle identification has been performed, we reevaluate the time differences $\delta_t(m)$, this time using for each track the mass assignment known from the cut on $d\delta_{t,e\pi}$ and subtracting the T_0 of the event. For the T_0 determination, the bunch crossing producing the event is evaluated as the integer part of the ratio $[\delta_t(e) + \delta_t(\pi)]/2T_{\rm bunch}$. We apply another TOF cut by selecting the events within the circle in the $\delta_t(e)$-$\delta_t(\pi)$ plane, as shown in Fig. 2 for MC events. This cut improves the background rejection by a factor of five, while eliminating 8% of the signal events at this analysis stage.

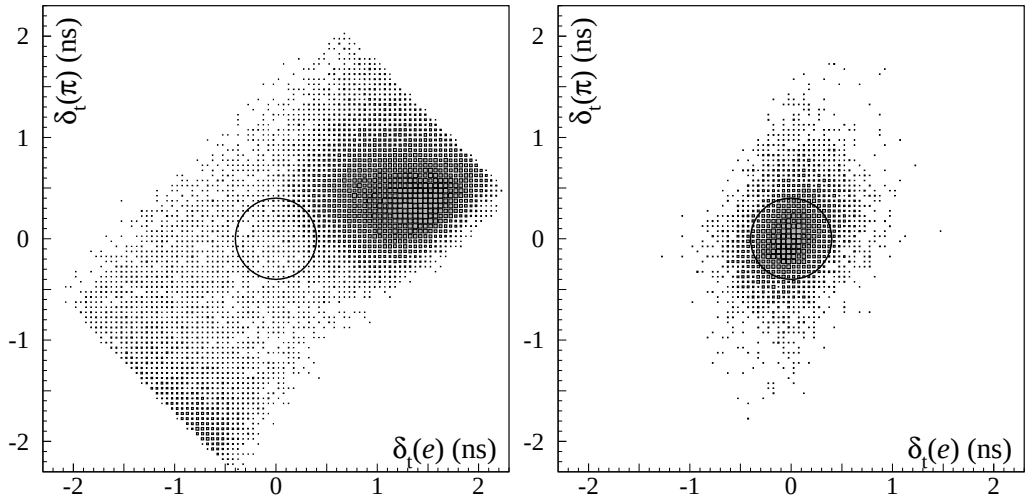

Fig. 2. Scatter plot of the time differences $\delta_t(\pi)$ vs $\delta_t(e)$ for π and e mass assignments for Monte Carlo events, for all K_S decays (left) and for $K_S \to \pi e\nu$ decays (right). Events within the circles are retained.

A powerful discriminating variable is the difference between the missing energy and momentum, $\Delta E_{\pi e} = E_{\rm miss} - p_{\rm miss}$, which is evaluated using the K_S momentum known from the K_L direction. For $\pi e\nu$ decays, $E_{\rm miss}$ and $p_{\rm miss}$ are the neutrino energy and momentum, and are equal. The distribution of $\Delta E_{\pi e}$ is shown in Fig. 3 after TOF cuts are imposed for $\pi^- e^+ \nu$ (left panel) and for $\pi^+ e^- \bar{\nu}$ (right panel) candidate events. A clear peak around zero is evident and corresponds to a clean signal for $K_S \to \pi e \nu$.

The residual background is dominated by $K_S \to \pi^+\pi^-(\gamma)$ decays. Events with $\Delta E_{\pi e} > 10\,\text{MeV}$ are mostly due to cases in which one pion decays to a muon before entering the tracking volume ("$\pi\mu$" events), in which the track identified as electron by TOF is badly reconstructed ("$\pi_{\rm bad}\pi$" events), or in which the radiated photon has an energy in the K_S frame above 7 MeV, thus shifting $M_{\pi\pi}$ below 490 MeV and $E_{\rm miss}$ toward positive values ("$\pi\pi\gamma$" events). Events with $\Delta E_{\pi e} < -10\,\text{MeV}$ are mostly "$\pi\mu$" or "$\pi_{\rm bad}\pi$" events, or are due to cases in which the track identified as the pion by TOF is badly reconstructed ("$\pi\pi_{\rm bad}$" events).

We discriminate between signal and residual background events by means of 5 kinematic variables: $\Delta E_{\pi e}$ itself; the difference $\mathrm{d_{PCA}}$ between the impact parameters of the two tracks with the IP; the difference $\Delta E_{\pi\pi}$ in the π-π hypothesis; the squared mass $M^2_{\rm trk}(e)$ of track 1(2) when it is identified as electron from TOF, calculated assuming that $p_S - p_{2(1)}$ is the momentum of an undetected pion and that $(p_S - p_1 - p_2)^2 = 0$; the energy $E^*_{\pi(e)}$ of the track identified as a π (e) from TOF, calculated in the K_S rest frame using the pion mass hypothesis.

Except for "$\pi\pi\gamma$" events, all of the background categories are characterized by poor vertex reconstruction quality, leading to a broad distribution of $\mathrm{d_{PCA}}$ as shown in Fig. 4, top left. In contrast, signal and "$\pi\pi\gamma$" events are peaked around zero. We discriminate "$\pi\mu$" events by the $M^2_{\rm trk}(e)$ variable, which peaks around m^2_μ, and "$\pi\pi\gamma$" events by the $\Delta E_{\pi\pi}$ variable, which peaks around zero. Finally, well reconstructed pion tracks from $K_S \to \pi^+\pi^-$ decays are identified by the value of E^*, which peaks around $m_K/2$, allowing us to recognize $\pi_{\rm bad}\pi$ or $\pi\pi_{\rm bad}$ events.

The number of events due to signal and to each of the background categories are evaluated through a global binned-likelihood fit using the above variables. Each event is assigned to one of five regions in the $\Delta E_{\pi e}$-$\mathrm{d_{PCA}}$ plane illustrated in Fig. 5. For each region, we use for the fit one of the variables defined above. The choice of the regions and the assignment of the fit variables to each region ensure good separation between each component in turn and all the others. In each region, the data are fit with the sum of the MC distributions in the appropriate variable for signal events and for events from each background source. The free parameters are the signal and background normalizations.

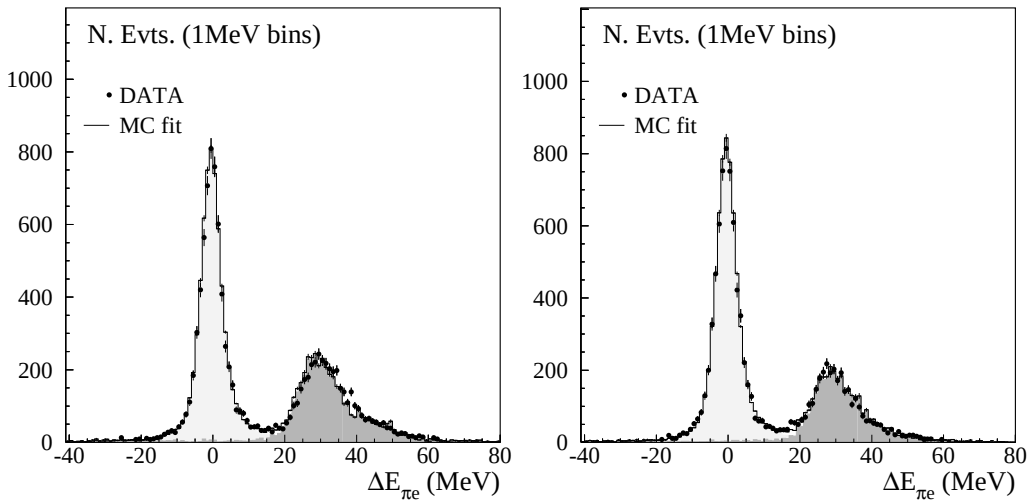

Fig. 3. $E_{\rm miss} - p_{\rm miss}$ spectrum for events selected as $\pi^- e^+ \nu$ (left panel) and $\pi^+ e^- \bar{\nu}$ (right panel). Filled dots represent data from the entire data set; the solid line is the result of a fit varying the normalization of MC distributions for signal (light gray) and background (dark gray), which are also shown.

For each source, the same normalization parameter is used in all fit regions.

The result of the fit is shown as the solid line in the distributions of Figs. 3 and 4. The MC simulations of $K_S \to \pi e \nu$ and $K_S \to \pi^+\pi^-$ decays include photon radiation in the final state [15]. If the effect of radiation were not taken into account, the result for the branching ratio would decrease by a few percent.

We perform two independent fits, one for each charge state. The estimated numbers of signal events are shown in Tab. 1. The quoted statistical errors include the contributions from fluctuations in the signal statistics, from the background subtraction, and from the finite MC statistics [16].

The systematic errors include the contribution from uncertainty in the shape of the signal distributions. In particular, we have studied in detail the reliability of the MC in reproducing the distribution of $\Delta E_{\pi e}$. We have compared data and MC resolutions obtained from samples of $K_S \to \pi^+\pi^-$ events tagged by the K_L crash, both for the momentum of each track and for the $\Delta E_{\pi\pi}$ variable. From these studies, we have extracted corrections to the MC resolutions for the tracking momentum and the polar and azimuthal angles for the K_L crash. After these corrections are applied, good agreement is observed for the core of the $\Delta E_{\pi e}$ distribution for signal events. In order to study the reliability of the simulation for the tails, an additional variable $x_{\rm PID}$ has been used to discriminate signal events. $x_{\rm PID}$ identifies $e^\pm$ tracks on the basis of the spatial distribution of the energy deposition in the EmC, and is independent from the track momenta used to obtain the fit variables. An alternative estimate of the number of signal events in each fit region is obtained from the $x_{\rm PID}$

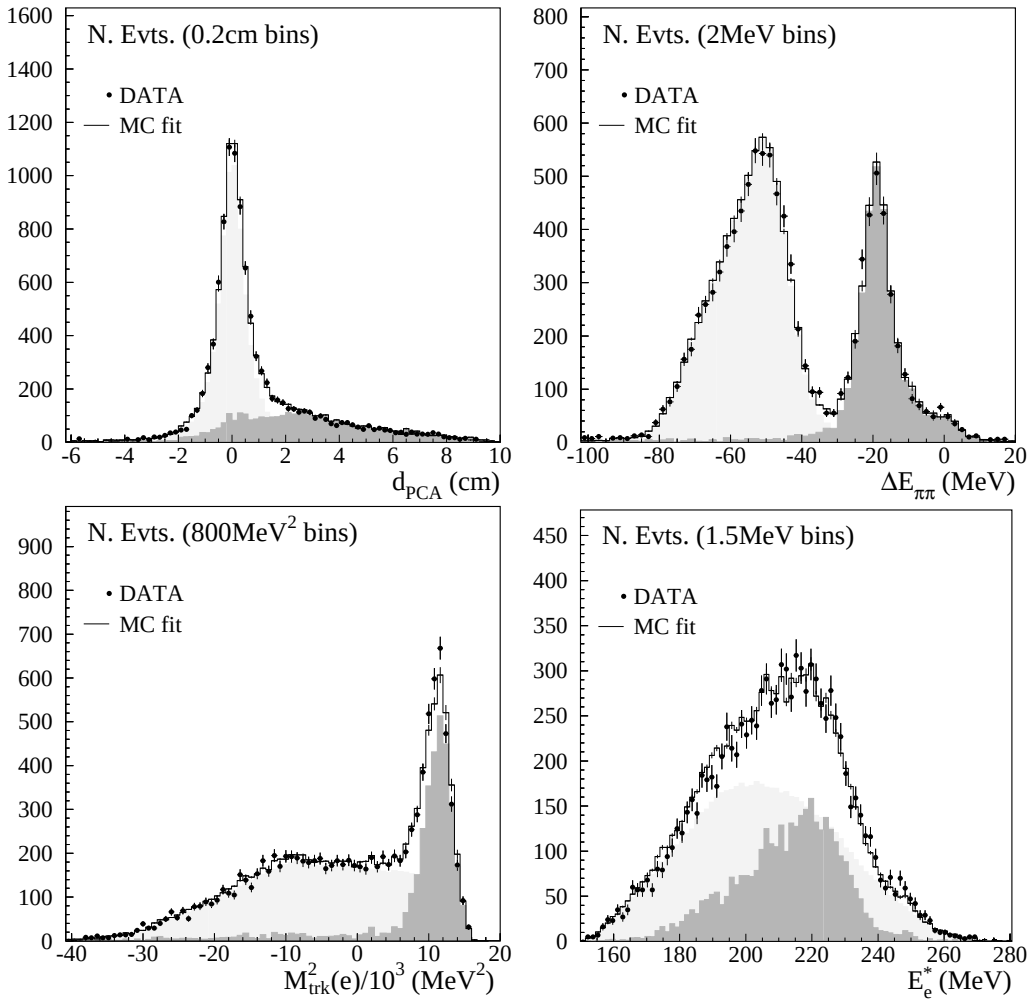

Fig. 4. Distributions for $\pi^+ e^- \bar{\nu}$ candidate events, for data (dots) and Monte Carlo events (solid line). Top left: d_{PCA} variable, peaking around zero for vertices of good quality (signal and $\pi\pi\gamma$ events); top right: $\Delta E_{\pi\pi}$, peaking around zero for $\pi\pi\gamma$ events; bottom left: $M^2_{\rm trk}(e)$, peaking around m^2_μ for $\pi\mu$ events; bottom right: E^*_e, peaking around $m_K/2$ for $\pi\pi_{\rm bad}$ events. In each plot, signal (light gray) and background (dark gray) contributions are also shown.

distribution, which is reliably reproduced by the MC simulation. Using this method, a significant difference in the number of signal events is observed only in regions 1 and 2, from which a shape correction is defined. This corresponds to a 0.5% correction to the final result, which is also taken as the corresponding systematic error.

The cut on the minimum cluster energy required for K_L-crash tagging dramatically affects the fraction of signal events in the tails of the $\Delta E_{\pi e}$ distribution: the looser the cut, the worse the resolution on the K_S momentum evaluated from the K_L direction. In order to check the robustness of the signal extraction, we have compared results obtained using three values for the minimum K_L cluster energy: 125 MeV, 200 MeV, and 300 MeV. The results obtained us-

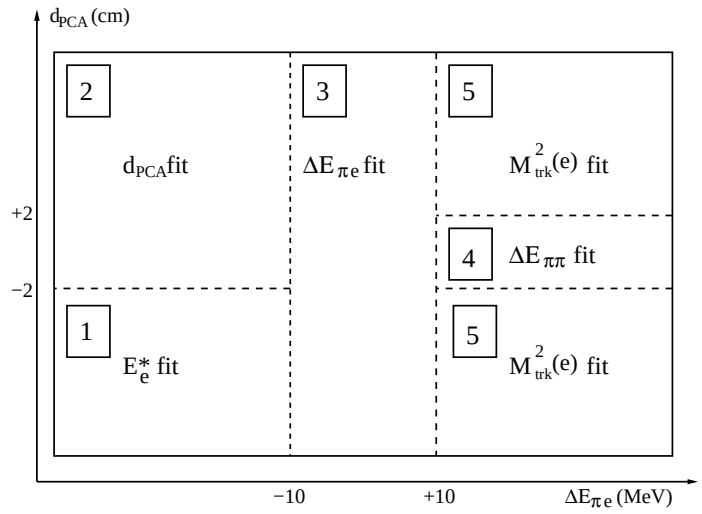

Fig. 5. Definition of the fit regions in the $\Delta E_{\pi e}$-$\mathrm{d_{PCA}}$ plane. In each region, the variable used for the fit is also specified.

ing independent samples are compatible with each other. The intermediate cut gives the minimum total uncertainty.

A detailed description of the fit procedure is given in Ref. 9.

4 Efficiency estimates

For both $K_S \to \pi^+\pi^-$ (normalization) and $K_S \to \pi e\nu$ (signal) events, we estimate the corrections for the geometrical acceptance and tagging and selection inefficiencies with the MC simulation. In order to account for data-MC differences, we weight each event with the ratio of the data and MC tracking efficiencies extracted from various control samples. We evaluate the probabilities for finding EmC clusters from K_S daughter particles and for satisfying the trigger conditions by combining data-extracted efficiencies, parametrized in terms of track momenta, with MC kinematics. For $K_S \to \pi e\nu$ events, we also use prompt $K_L \to \pi e\nu$ decays tagged by $K_S \to \pi^+\pi^-$ as a data control sample for efficiency evaluation. With this method, we obtain alternative estimates for the trigger and cluster efficiencies and evaluate the corrections for vertex reconstruction and π-e TOF identification inefficiencies. These methods are described in detail in Refs. 9 and 17.

For $K_S \to \pi e\nu$ decays, the efficiencies are determined separately for each charge state and for the 2001 and 2002 data. We summarize the results for the overall efficiencies, given the tag requirement, in Tab. 2. The differences between the efficiencies for the two charge states arise from the different re-

K_S decay	Selection efficiency	
	Year 2001	Year 2002
$\pi^+\pi^-$	$0.5954 \pm 0.0004_{\rm stat} \pm 0.0010_{\rm syst}$	$0.6035 \pm 0.0004_{\rm stat} \pm 0.0010_{\rm syst}$
$\pi^-e^+\nu$	$0.2139 \pm 0.0019_{\rm stat} \pm 0.0014_{\rm syst}$	$0.2197 \pm 0.0012_{\rm stat} \pm 0.0021_{\rm syst}$
$\pi^+e^-\bar{\nu}$	$0.2252 \pm 0.0016_{\rm stat} \pm 0.0009_{\rm syst}$	$0.2328 \pm 0.0011_{\rm stat} \pm 0.0011_{\rm syst}$

Table 2
Selection efficiencies for $K_S \to \pi^+\pi^-$ and $K_S \to \pi e\nu$ decays, for the 2001 and 2002 data sets, given the K_L-crash tag.

sponse of the calorimeter to π^+ and π^-, influencing the cluster, trigger, and TOF efficiencies. The uncertainties on the tracking and cluster/trigger efficiencies contribute approximately equally to the systematic errors on the overall efficiencies. A variation in the cluster/trigger efficiencies between 2001 and 2002 is reflected in the values for the overall efficiencies. The corresponding systematic errors have been estimated from the comparison of the results obtained using prompt $K_L \to \pi e\nu$ decays and using single-particle weights to correct the MC. The difference between the results obtained with the two methods is larger for $\pi^-e^+\nu$ events, and for the 2002 data.

In principle, the K_L-crash identification efficiency cancels out in the ratio of the number of selected $K_S \to \pi e\nu$ and $K_S \to \pi^+\pi^-$ events. In practice, since the event T_0 is obtained from the K_S and the K_L is recognized by its time of flight, there is a small dependence of the K_L-crash identification efficiency on the K_S decay mode. A correction for this effect is obtained by studying the accuracy of the T_0 determination in each case [9,17,18]. The ratio $R_{\rm tag}$ of the tagging efficiencies for $K_S \to \pi e\nu$ and $K_S \to \pi^+\pi^-$ is found to differ from unity by $\sim$1%. This effect is included in the efficiency values shown in Tab. 2.

5 Results

For each charge state and for the data set for each year, we obtain the ratio of BR's by normalizing the number of signal events to the number of $K_S \to \pi^+\pi^-$ events and correcting for the overall selection efficiencies:

$$\frac{\Gamma(K_S \to \pi^\mp e^\pm \nu(\overline{\nu}))}{\Gamma(K_S \to \pi^+\pi^-)} = \frac{N(\pi^\mp e^\pm \nu(\overline{\nu}))}{N(\pi\pi)} \times \frac{\epsilon^{\pi\pi}_{\rm tot}}{\epsilon^{\pm}_{\rm tot}}.$$

The results for the BR's from the data sets for each year are compatible with probabilities greater than 50%. Averaging the results obtained for each data

set, we obtain the following results:

$$\begin{aligned} R_{e+} &\equiv \frac{\Gamma(K_S \to \pi^- e^+ \nu)}{\Gamma(K_S \to \pi^+\pi^-)} = (5.099 \pm 0.082_{\rm stat} \pm 0.039_{\rm syst}) \times 10^{-4} \\ R_{e-} &\equiv \frac{\Gamma(K_S \to \pi^+ e^- \bar{\nu})}{\Gamma(K_S \to \pi^+\pi^-)} = (5.083 \pm 0.073_{\rm stat} \pm 0.042_{\rm syst}) \times 10^{-4} \\ R_{e} &\equiv \frac{\Gamma(K_S \to \pi e \nu)}{\Gamma(K_S \to \pi^+\pi^-)} = (10.19 \pm 0.11_{\rm stat} \pm 0.07_{\rm syst}) \times 10^{-4} \end{aligned} \quad (6)$$

To obtain the value of the ratio $\mathrm{BR}(K_S \to \pi e\nu)/\mathrm{BR}(K_S \to \pi^+\pi^-)$ we take into account the correlation between the values measured for the two charge modes. This correlation arises from uncertainties on the shapes of the signal distributions in the fit variables that are common to both charge states; the correlation parameter is 13%.

The charge asymmetry of Eq. (1) is given by:

$$A_S = \frac{N(\pi^- e^+ \nu)/\epsilon^+_{\rm tot} - N(\pi^+ e^- \bar{\nu})/\epsilon^-_{\rm tot}}{N(\pi^- e^+ \nu)/\epsilon^+_{\rm tot} + N(\pi^+ e^- \bar{\nu})/\epsilon^-_{\rm tot}}.$$

Combining the results for all data, we obtain:

$$A_S = (1.5 \pm 9.6_{\rm stat} \pm 2.9_{\rm syst}) \times 10^{-3}.$$

In order to perform a stability test, we have divided the entire data set into 17 samples and performed the analysis individually for each sample. Values of χ^2 corresponding to probabilities above 50% are observed for all of the measured quantities [9].

The various contributions to the total fractional error on $\mathrm{BR}(K_S \to \pi e\nu)$ and to the total error on A_S are listed in Tabs. 3 and 4. For the measurement of the BR, the uncertainty on the signal count from fit systematics is the dominant contribution to the total systematic error.

For the purposes of measuring the dependence of the form factor $f_+(t)/f_+(0)$ on the 4-momentum transfer squared $t = (P_K - P_\pi)^2$, the elimination of background from the sample while preserving statistics is a more important consideration than the understanding of the selection efficiencies at the level required in the branching-ratio analysis. We therefore use slightly different selection criteria to isolate a clean sample of $K_S \to \pi e\nu$ events: we require $|\Delta E_{\pi e}| < 10\,\mathrm{MeV}$ and cut on the quality of the K_S vertex. In order to limit loss of statistics, we loosen the energy requirement on the K_L crash to 125 MeV. We select about 15 000 signal events, combining the data for the two years and charge modes. With this selection, the bacgkround contamination is reduced to 0.7%. Because of the limited statistics, we only measure the slope parameter of the form factor in the linear approximation, $f_+(t)/f_+(0) = 1 + \lambda_+ t/m_\pi^2$. More

	Fractional error (10^{-3})	
	Statistical	Systematic
Statistics of $K_S \to \pi e\nu$	9.1	
Statistics of $K_S \to \pi^+\pi^-$	0.1	
Preselection efficiency, $K_S \to \pi e\nu$	1.5	2.9
Trigger efficiency, $K_S \to \pi e\nu$	0.2	0.3
TOF efficiency, $K_S \to \pi e\nu$	2.3	
Fit systematics, $K_S \to \pi e\nu$		6.2
Preselection efficiency, $K_S \to \pi^+\pi^-$	0.3	1.6
Trigger efficiency, $K_S \to \pi^+\pi^-$	0.1	0.8
Ratio of tagging efficiencies	5.0	
Ratio of cosmic veto inefficiencies	1.0	
Total	10.8	7.1
Total fractional error	**12.9**	

Table 3
Contributions to the fractional error on BR($K_S \to \pi e\nu$)/BR($K_S \to \pi^+\pi^-$).

	Error (10^{-3})	
	Statistical	Systematic
Statistics of $K_S \to \pi e\nu$	9.1	
Preselection efficiency, $K_S \to \pi e\nu$	1.5	2.9
Trigger efficiency, $K_S \to \pi e\nu$	0.1	0.3
TOF efficiency, $K_S \to \pi e\nu$	2.3	
Fit systematics, $K_S \to \pi e\nu$		0.4
Tagging efficiencies	0.4	
Cosmic veto inefficiencies	1.0	
Total	9.6	2.9
Total error	**10.0**	

Table 4
Contributions to the absolute error on A_S.

precisely, we fit the ratio of data and MC distributions in $t/m^2_{\pi+}$ with the function:

$$F(t) = A \times \left(\frac{1 + \lambda_+ t/m^2_{\pi+}}{1 + \lambda_{+,MC} t/m^2_{\pi+}} \right)^2 ,$$

where A and λ_+ are the free parameters of the fit, and $\lambda_{+,MC} = 0.03$ is the value of the slope used in the MC generation. Effects from the finite resolution on t are negligible with respect to the statistical error and are ignored. We find $\lambda_+ = (33.9 \pm 4.1) \times 10^{-3}$ with $\chi^2/\text{dof} = 12.9/11$, corresponding to a probability $P(\chi^2) \simeq 30\%$. This result is in reasonable agreement with the value of λ_+ for semileptonic K_L and K^+ decays, $(28.82 \pm 0.34) \times 10^{-3}$, from the average of results from KTeV [19], ISTRA+ [20], NA48 [21], and KLOE. [22].

6 Interpretation of the results

6.1 Determination of absolute BR's

In order to evaluate the BR's for the semileptonic modes, we combine the ratios of BR's measured for each charge [Eq. (6)] with the most precise measurement of the ratio

$$R = \frac{\Gamma(K_S \to \pi^+\pi^-)}{\Gamma(K_S \to \pi^0\pi^0)} = 2.236 \pm 0.015, \tag{7}$$

which was also obtained at KLOE [23]. The only remaining mode with a BR large enough to measurably affect the constraint $\sum_f \mathrm{BR}(K_S \to f) = 1$ is $K_{\mu 3}$; the BR's for all other channels sum up to $\sim 10^{-5}$. Assuming lepton universality, we have

$$r_{\mu e} = \frac{\Gamma\left(K_S \to \pi\mu\nu\right)}{\Gamma\left(K_S \to \pi e\nu\right)} = \frac{1+\delta_K^\mu}{1+\delta_K^e}\frac{I_K^\mu}{I_K^e}, \tag{8}$$

where $\delta_K^{\mu,e}$ are mode-dependent long-distance radiative corrections and $I_K^{\mu,e}$ are decay phase-space integrals. Using $I_K^\mu/I_K^e = 0.6622(18)$ from KTeV [24] and $(1+\delta_K^\mu)/(1+\delta_K^e) = 1.0058(10)$ from Ref. 25, we get $r_{\mu e} = 0.6660(19)$. We evaluate the four main BR's of the K_S from

$$\mathrm{BR}(K_S \to i) = \frac{\Gamma(K_S \to i)/\Gamma(K_S \to \pi^+\pi^-)}{1 + 1/R + (R_{e+} + R_{e-})(1 + r_{\mu e})}, \tag{9}$$

where $i = \pi^+\pi^-$, $\pi^0\pi^0$, $\pi^- e^+ \nu$, $\pi^+ e^- \bar{\nu}$. We find:

$$\begin{aligned}
\mathrm{BR}(K_S \to \pi^+\pi^-) &= (69.02 \pm 0.14) \times 10^{-2} \\
\mathrm{BR}(K_S \to \pi^0\pi^0) &= (30.87 \pm 0.14) \times 10^{-2} \\
\mathrm{BR}(K_S \to \pi^- e^+ \nu) &= (3.519 \pm 0.063) \times 10^{-4} \\
\mathrm{BR}(K_S \to \pi^+ e^- \bar{\nu}) &= (3.508 \pm 0.058) \times 10^{-4}
\end{aligned} \tag{10}$$

The correlation matrix $\langle \delta_i \delta_j \rangle / \sqrt{\langle \delta_i^2 \rangle \langle \delta_j^2 \rangle}$ is:

$$\begin{array}{c} \\ \pi^+\pi^- \\ \pi^0\pi^0 \\ \pi^- e^+ \nu \\ \pi^+ e^- \overline{\nu} \end{array}
\begin{array}{c}
\begin{array}{cccc} \pi^+\pi^- & \pi^0\pi^0 & \pi^- e^+ \nu & \pi^+ e^- \overline{\nu} \end{array} \\
\left(\begin{array}{cccc}
1 & -0.9999 & 0.1106 & 0.1196 \\
-0.9999 & 1 & -0.1187 & -0.1272 \\
0.1106 & -0.1187 & 1 & 0.1445 \\
0.1196 & -0.1272 & 0.1445 & 1
\end{array} \right)
\end{array} \tag{11}$$

The contribution from the error on $r_{\mu e}$ is included in the systematic errors. Taking correlations into account, we have:

$$\mathrm{BR}(K_S \to \pi e \nu) = (7.028 \pm 0.092) \times 10^{-4}. \tag{12}$$

6.2 Test of the $\Delta S = \Delta Q$ rule

From the total BR we test the validity of the $\Delta S = \Delta Q$ rule in CPT-conserving transitions [Eq. (4)]. We use the following values for the K_S and K_L lifetimes: $\tau_S = 0.08958(6)\,\mathrm{ns}$ from the PDG [13] and $\tau_L = 50.84(23)\,\mathrm{ns}$ from recent measurements from KLOE [26, 27]. For $\mathrm{BR}(K_L \to \pi e \nu)$, we use the value from KLOE, 0.4007(15) [26]. We obtain:

$$\mathrm{Re}\, x_+ = (-1.2 \pm 3.6) \times 10^{-3}. \tag{13}$$

The error on this value represents an improvement by almost a factor of two with respect to the most precise previous measurement, that from the CPLEAR experiment [5].

6.3 Test of the CPT symmetry

From the sum and difference of the K_L and K_S charge asymmetries one can test for possible violations of the CPT symmetry, either in the decay amplitudes or in the mass matrix [Eqs. (2) and (3)]. Using $A_L = (3.34 \pm 0.07) \times 10^{-3}$ [13], we obtain from Eq. (2)

$$\mathrm{Re}\, x_- + \mathrm{Re}\, \delta = (-0.5 \pm 2.5) \times 10^{-3}. \tag{14}$$

Current knowledge of these two parameters is dominated by results from CPLEAR [3]: the error on $\mathrm{Re}\,\delta$ is 3×10^{-4} and that on $\mathrm{Re}\, x_-$ is 10^{-2}. Using $\mathrm{Re}\,\delta = (3.0 \pm 3.3_{\mathrm{stat}} \pm 0.6_{\mathrm{syst}}) \times 10^{-4}$ from CPLEAR, we obtain:

$$\mathrm{Re}\, x_- = (-0.8 \pm 2.5) \times 10^{-3}, \tag{15}$$

thus improving on the error of $\mathrm{Re}\, x_-$ by a factor of five.

From Eq. (3) we obtain

$$\mathrm{Re}\,\epsilon - \mathrm{Re}\, y = (1.2 \pm 2.5) \times 10^{-3}. \tag{16}$$

We calculate $\mathrm{Re}\,\epsilon$ using values from Ref. 13 that are obtained without assuming CPT conservation: $\mathrm{Re}\,\epsilon = |\epsilon| \times \cos\phi_\epsilon = (1.62 \pm 0.04) \times 10^{-3}$. Subtracting this value from Eq. (16), we find

$$\mathrm{Re}\, y = (0.4 \pm 2.5) \times 10^{-3}, \tag{17}$$

which has precision comparable to that (3×10^{-3}) obtained from the unitarity relation by CPLEAR [4].

6.4 Determination of V_{us}

The value of V_{us} can be extracted from the measurement of $\mathrm{BR}(K_S \to \pi e\nu)$ and from the K_S lifetime, τ_S:

$$V_{us} \times f_+^{K^0\pi^-}(0) = \left[\frac{128\,\pi^3\,\mathrm{BR}(K_S \to \pi e\nu)}{\tau_S\, G_\mu^2\, M_K^5\, S_{\mathrm{ew}}\, I_K(\lambda_+, 0)}\right]^{1/2} \frac{1}{1+\delta_{\mathrm{em}}^K}, \qquad (18)$$

where $f_+^{K^0\pi^-}(0)$ is the vector form factor at zero momentum transfer and $I_K(\lambda_+, 0)$ is the result of the phase space integration after factoring out $f_+^{K^0\pi^-}(0)$; both quantities are evaluated in absence of radiative corrections. The radiative corrections [25, 28] for the form factor and the phase-space integral are included via the parameter $\delta_{\mathrm{em}}^K = (0.55 \pm 0.10)\times10^{-2}$ [28]. The short-distance electroweak corrections are included in the parameter $S_{\mathrm{ew}} = 1.0232$ [29].

The pole parametrization of the vector form factor is $f_+(t) = f_+(0)[M_V^2/(M_V^2 - t)]$. Expanding this expression to second order gives $\lambda_+'' = 2\lambda_+'^2$, where λ_+' and λ_+'' are the linear and quadratic slopes,

$$f_+(t) = f_+(0)\left[1 + \lambda_+'\frac{t}{m_{\pi^+}^2} + \frac{\lambda_+''}{2}\frac{t^2}{m_{\pi^+}^4}\right].$$

We evaluate the phase space integral from the value of M_V from KLOE, $M_V = 870.0 \pm 9.2\,\mathrm{MeV}$ [22], and get $I_K = 0.10320 \pm 0.00020$. The pole fit result is less affected by the strong correlation between the linear and quadratic slopes and provides better consistency among the values of I_K from different experiments (KLOE [22], KTeV [19], ISTRA+ [20, 30], and NA48 [21]) than is obtained using the results for λ_+' and λ_+''.

We obtain:

$$f_+^{K^0\pi^-}(0) \times V_{us} = 0.2150 \pm 0.0014 \qquad (19)$$

Using $f_+^{K^0\pi^-}(0) = 0.961 \pm 0.008$ from Ref. 31 (this value is in agreement with a recent lattice calculation [32]), we get

$$V_{us} = 0.2238 \pm 0.0024. \qquad (20)$$

To perform a test of first-row CKM unitarity, we define:

$$\Delta = 1 - V_{ud}^2 - V_{us}^2 - V_{ub}^2$$

Using $V_{ud}=0.97377\pm0.00027$ from Ref. 33 and including the small contribution of V_{ub} [13], we obtain

$$\Delta = (1.7 \pm 1.2) \times 10^{-3}, \tag{21}$$

which is compatible (1.4 σ) with zero.

A new measurement of R has recently been made at KLOE, with a precision improved by more than a factor of two with respect to Eq. 7. Combining the new and old KLOE measurements, we obtain $R= 2.2549 \pm 0.0054$. The results presented in Eqs. 10, 12, 13, 19, 20, and 21 depend only slightly on the value used for R. The results obtained using the updated value of R are listed below:

$$\begin{aligned}
\mathrm{BR}(K_S \to \pi^+\pi^-) &= (69.196 \pm 0.051) \times 10^{-2} \\
\mathrm{BR}(K_S \to \pi^0\pi^0) &= (30.687 \pm 0.051) \times 10^{-2} \\
\mathrm{BR}(K_S \to \pi^- e^+ \nu) &= (3.528 \pm 0.062) \times 10^{-4} \\
\mathrm{BR}(K_S \to \pi^+ e^- \bar{\nu}) &= (3.517 \pm 0.058) \times 10^{-4} \\
\mathrm{BR}(K_S \to \pi e \nu) &= (7.046 \pm 0.091) \times 10^{-4}
\end{aligned} \tag{22}$$

From the last of these, the following quantities follow:

$$\begin{aligned}
\mathrm{Re}\, x_+ &= (-0.5 \pm 3.6) \times 10^{-3} \\
f_+^{K^0\pi^-}(0) \times V_{us} &= 0.2153 \pm 0.0014 \\
V_{us} &= 0.2240 \pm 0.0024 \\
\Delta &= (1.6 \pm 1.2) \times 10^{-3}
\end{aligned} \tag{23}$$

The differences between these quantities when calculated using the old and new values of R are well within the stated uncertainties.

Acknowledgements

We thank the DAΦNE team for their efforts in maintaining low-background running conditions and their collaboration during all data taking. We also thank F. Fortugno for his efforts in ensuring good operations of the KLOE computing facilities and F. Mescia and G. Isidori for their help. This work was supported in part by DOE grant DE-FG-02-97ER41027; by EURODAPHNE, contract FMRX-CT98-0169; by the German Federal Ministry of Education and Research (BMBF) contract 06-KA-957; by Graduiertenkolleg 'H.E. Phys. and Part. Astrophys.' of Deutsche Forschungsgemeinschaft, Contract No. GK 742; by INTAS, contracts 96-624, 99-37.

References

[1] M. Ademollo, R. Gatto, Phys. Rev. Lett. 13 (1964) 264.

[2] KTeV Collaboration, A. Alavi-Harati *et al.*, Phys. Rev. Lett. 88 (2002) 181601.

[3] CPLEAR Collaboration, A. Angelopoulos, *et al.*, Phys. Lett. B444 (1998) 52.

[4] CPLEAR Collaboration, A. Apostolakis, *et al.*, Phys. Lett. B456 (1999) 297.

[5] CPLEAR Collaboration, A. Angelopoulos, *et al.*, Phys. Lett. B444 (1998) 38.

[6] KLOE Collaboration, A. Aloisio, *et al.*, Phys. Lett. B535 (2002) 37.

[7] KLOE Collaboration, M. Adinolfi, *et al.*, Nucl. Instr. and Meth. A488 (2002) 51.

[8] KLOE Collaboration, M. Adinolfi, *et al.*, Nucl. Instr. and Meth. A482 (2002) 363.

[9] C. Gatti, T. Spadaro, KLOE Note 208 (2006), unpublished.
URL `http://www.lnf.infn.it/kloe/pub/knote/kn208.ps`

[10] KLOE Collaboration, M. Adinolfi, *et al.*, Nucl. Instr. and Meth. A492 (2002) 134.

[11] N. Paver, Riazuddin, Phys. Lett. B246 (1990) 240.

[12] N. Brown, F. E. Close, Scalar mesons and kaons in ϕ radiative decay & their implications for studies of CP violation at DAΦNE, in: L. Maiani, G. Pancheri, N. Paver (Eds.), The DAΦNE Physics Handbook, Vol. 2, 1992, p. 447.

[13] S. Eidelman, *et al.*, Particle Data Group, Phys. Lett. B592, and 2005 partial update for edition 2006.
URL `http://pdg.lbl.gov`

[14] KLOE Collaboration, F. Ambrosino, *et al.*, Precise measurement of $\Gamma(K_S \to \pi^+\pi^-)/\Gamma(K_S \to \pi^0\pi^0)$ with the KLOE detector at DAΦNE, **hep-ex/0601025**.

[15] C. Gatti, Eur. Phys. J. C45 (2005) 417, and references therein.

[16] R. J. Barlow, C. Beeston, Comput. Phys. Commun. 77 (1993) 219.

[17] C. Gatti, T. Spadaro, KLOE Note 176 (2002), unpublished.
URL `http://www.lnf.infn.it/kloe/pub/knote/kn176.ps.gz`

[18] C. Gatti, M. Palutan, T. Spadaro, KLOE Note 209 (2006), unpublished.
URL `http://www.lnf.infn.it/kloe/pub/knote/kn209.ps`

[19] KTeV Collaboration, T. Alexopoulos, *et al.*, Phys. Rev. D70 (2004) 092007.

[20] O. P. Yushchenko, et al., Phys. Lett. B589 (2004) 111.

[21] NA48 Collaboration, A. Lai, *et al.*, Phys. Lett. B604 (2004) 1.

[22] KLOE Collaboration, F. Ambrosino, *et al.*, Measurement of the form-factor slopes for the decay $K_L \to \pi e\nu$ with the KLOE detector **hep-ex/0601038**, accepted for publication by Phys. Lett. B.

[23] KLOE Collaboration, A. Aloisio *et al.*, Phys. Lett. B538 (2002) 21.

[24] KTeV Collaboration, T. Alexopoulos, *et al.*, Phys. Rev. D70 (2004) 092007.

[25] T. C. Andre, Radiative corrections to K0(l3) decays, **hep-ph/0406006**.

[26] KLOE Collaboration, F. Ambrosino, *et al.*, Phys. Lett. B632 (2006) 43.

[27] KLOE Collaboration, F. Ambrosino, *et al.*, Phys. Lett. B626 (2005) 15.

[28] V. Cirigliano, H. Neufeld, H. Pichl, Eur. Phys. J. C35 (2004) 53.

[29] W. J. Marciano, A. Sirlin, Phys. Rev. Lett. 71 (1993) 3629.

[30] O. P. Yushchenko, et al., Phys. Lett. B581 (2004) 31.

[31] H. Leutwyler, M. Roos, Z. Phys. C25 (1984) 91.

[32] D. Becirevic, et al., Nucl. Phys. B705 (2005) 339.

[33] W. J. Marciano, A. Sirlin, Phys. Rev. Lett. 96 (2006) 032002.